

## Article

# Simultaneous Anaerobic Ammonium Oxidation and Electricity Generation in Microbial Fuel Cell: Performance and Electrochemical Characteristics

Jiqiang Zhang <sup>1,2</sup>, Zaiwang Zhang <sup>1</sup>, Kun Rong <sup>1</sup>, Haiying Guo <sup>1</sup>, Jing Cai <sup>2,3</sup>, Yajuan Xing <sup>2,4</sup>, Lili Ren <sup>1</sup>, Jiajun Ren <sup>1</sup>, Tao Wu <sup>1</sup>, Jialiang Li <sup>1,\*</sup> and Ping Zheng <sup>2,\*</sup>

<sup>1</sup> Shandong Engineering and Technology Research Center for Ecological Fragile Belt of Yellow River Delta, School of Biological & Environmental Engineering, Binzhou University, Binzhou 256600, China

<sup>2</sup> Department of Environmental Engineering, Zhejiang University, Hangzhou 310058, China

<sup>3</sup> College of Environmental Science and Engineering, Zhejiang Gongshang University, Hangzhou 310058, China

<sup>4</sup> School of Geomatics and Municipal Engineering, Zhejiang University of Water Resources and Electric Power, Hangzhou 310058, China

\* Correspondence: [ljliang@bzu.edu.cn](mailto:ljliang@bzu.edu.cn) (J.L.); [pzheng@zju.edu.cn](mailto:pzheng@zju.edu.cn) (P.Z.)

**Abstract:** In this study, a microbial fuel cell (MFC) that can achieve simultaneous anode anaerobic ammonium oxidation (anammox) and electricity generation (anode anammox MFC) by high-effective anammox bacteria fed with purely inorganic nitrogen media was constructed. As the influent concentrations of ammonium ( $\text{NH}_4^+ \text{-N}$ ) and nitrite ( $\text{NO}_2^- \text{-N}$ ) gradually increased from 25 to 250 mg/L and 33–330 mg/L, the removal efficiencies of  $\text{NH}_4^+ \text{-N}$ ,  $\text{NO}_2^- \text{-N}$  and TN were over 90%, 90% and 80%, respectively, and the maximum volumetric nitrogen removal rate reached  $3.01 \pm 0.27 \text{ kgN}/(\text{m}^3 \cdot \text{d})$ . The maximum voltage and maximum power density were  $225.48 \pm 10.71 \text{ mV}$  and  $1308.23 \pm 40.38 \text{ mW/m}^3$ , respectively. Substrate inhibition took place at high nitrogen concentrations ( $\text{NH}_4^+ \text{-N} = 300 \text{ mg/L}$ ,  $\text{NO}_2^- \text{-N} = 396 \text{ mg/L}$ ). Electricity production performance significantly depended upon the nitrogen removal rate under different nitrogen concentrations. The reported low coulombic efficiency (CE, 4.09–5.99%) may be due to severe anodic polarization. The anode charge transfer resistance accounted for about 90% of the anode resistance. The anode process was the bottleneck for energy recovery and should be further optimized in anode anammox MFCs. The high nitrogen removal efficiency with certain electricity recovery potential in the MFCs suggested that anode anammox MFCs may be used in energy sustainable nitrogen-containing wastewater treatment.



**Citation:** Zhang, J.; Zhang, Z.; Rong, K.; Guo, H.; Cai, J.; Xing, Y.; Ren, L.; Ren, J.; Wu, T.; Li, J.; et al. Simultaneous Anaerobic Ammonium Oxidation and Electricity Generation in Microbial Fuel Cell: Performance and Electrochemical Characteristics. *Processes* **2022**, *10*, 2379. <https://doi.org/10.3390/pr10112379>

Academic Editors: Dimitris Zagklis and Georgios Bampos

Received: 20 October 2022

Accepted: 9 November 2022

Published: 12 November 2022

**Publisher's Note:** MDPI stays neutral with regard to jurisdictional claims in published maps and institutional affiliations.



**Copyright:** © 2022 by the authors. Licensee MDPI, Basel, Switzerland. This article is an open access article distributed under the terms and conditions of the Creative Commons Attribution (CC BY) license (<https://creativecommons.org/licenses/by/4.0/>).

## 1. Introduction

Traditional wastewater treatment is an energy-intensive process and has received considerable attention due to the pressure of carbon neutralization and energy shortage, so it is of great necessity to reduce energy consumption in this process [1,2]. As a matter of fact, substantial internal chemical energy is contained in water pollutants, and the wastewater may contain 9.3 times as much energy as is used to treat it [3]. As a promising technology for sustainable wastewater treatment, microbial fuel cells (MFC) can use these pollutants as fuels and directly convert the chemical energy into electricity with microorganisms as catalysts [4]. In theory, it is feasible to turn wastewater treatment into a self-sustaining, or even a net energy-producing, process by MFCs [1,5,6].

MFCs generate electricity by harvesting the electrons donated to the anode from fuel oxidation [7]. Various pollutants from wastewater and pure chemical compounds have been examined as fuel in MFCs [8,9]. A large number of studies have been conducted on the oxidation of most ubiquitous organic pollutants in wastewater to produce electric power (organic MFCs). However, nutrient removal remains a significant challenge in

efficient wastewater treatment with MFCs and emerging studies have mainly focused on energy-containing nitrogen pollutants [10–12]. As one of the most common inorganic water pollutants, ammonium can also be used as the fuel in MFCs [13]. Anode nitrification MFCs represent one type of MFCs based on the nitrification process, involving aerobic oxidation of ammonium as the main reaction for anode ammonium oxidation [13,14]. Electricity can be acquired from anode nitrification MFCs, but the oxidation of ammonium by nitrifying bacteria requires oxygen supply. The presence of oxygen would hamper extracellular electron transfer and greatly decrease power generation in the MFCs [13–15]. If oxygen can be removed from the anode ammonium oxidation process, more electric energy might be recovered via the harvesting of the internal chemical energy stored in ammonium.

Anaerobic ammonium oxidation (anammox), a process in which ammonium is oxidized by anammox bacteria that take nitrite as an electron acceptor ( $\text{NH}_4^+ + \text{NO}_2^- \rightarrow \text{N}_2 + 2\text{H}_2\text{O}$ ), is known as a low-cost and eco-friendly nitrogen removal method [16,17]. As a result, the combination of the anammox process and MFCs (anode anammox MFCs) might have several advantages over the anode nitrification MFCs. First, ammonium can be oxidized without oxygen, which leads to less electron loss. On the other hand, the anammox process has a significantly higher ammonium oxidation rate than that of the nitrification process [18,19], implying that it involves faster electron transfer in electricity generation. The possibility of MFCs with simultaneous anode anammox and electricity generation abilities has been verified in several studies [20,21]. However, little evidence is available for the ways in which anammox bacteria, as exoelectrogens, can limit the development of anode anammox MFCs. A recent report concluded that anammox bacteria are a newly discovered type of electrochemically active bacteria in microbial electrolysis cells (MECs) and that anode anammox MFCs have broad prospects for application in this field [22]. Electrogenesis bacteria are the core of the MFC system [1,5]. In addition, highly effective electrochemically active bacteria would be the key for the improvement of these promising anode anammox MFCs with great functions in pollutant removal and electricity generation. In a previous study, a high-loaded anammox reactor reached an anammox rate of  $76.7 \text{ kg N}/(\text{m}^3 \cdot \text{d})$  [18]. Exploring the potential of nitrogen removal and electricity generation using anammox bacteria with such high activity in MFCs would improve our understanding of the bioelectrochemical processes in anode anammox MFCs.

In the present study, anammox bacteria from the highly loaded anammox reactor were collected as the anode inoculum to construct the anode anammox MFC, and the MFC was fed with purely inorganic nitrogen media. The objectives of the present study were to investigate the nitrogen removal and the electricity generation performance of the anode anammox MFC, and develop a better understanding of the electrochemical characteristics of this bioelectrochemical process.

## 2. Materials and Methods

### 2.1. Construction of the Anode Anammox MFCs

The anode anammox MFC was a dual chamber MFC (Figure 1). The anode and cathode chamber both had a net volume of 400 mL with graphite felt (8 cm × 4 cm × 0.5 cm, Liaoyang Jingu Carbon Fiber Technology Co., Ltd., Liaoyang, China) as electrodes, separated by cation exchange membranes (CEM, Φ 6 cm, Membranes International, Ringwood, NJ, USA). The electrodes were fixed in the center of the anode and cathode chamber by stainless steel wires. A  $1000 \Omega$  resistor was connected to the electrodes with copper wires to form a closed circuit. The output voltage was monitored by a data acquisition system (DAS, Agilent 34970A, Agilent Technologies, Santa Clara, CA, USA).

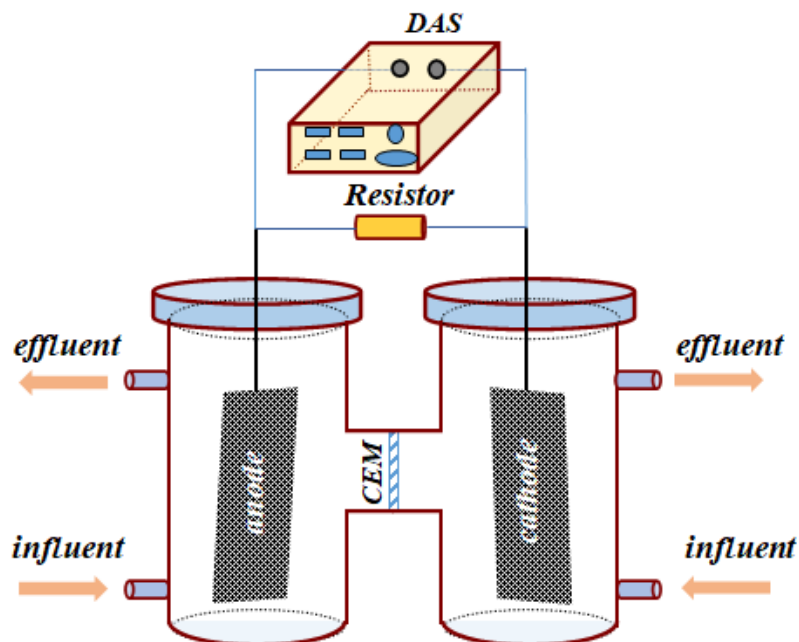


**Figure 1.** Schematic diagram of the anode anammox MFC.

## 2.2. Operating Conditions

The anode inoculum (highly effective anammox bacteria) was taken from a highly loaded anammox reactor in our lab [18]. The synthetic wastewater contained  $(\text{NH}_4)_2\text{SO}_4$  and  $\text{NaNO}_2$  and other trace components. The trace element solution was the same as in our previous study [23]. The ammonium ( $\text{NH}_4^+$ -N) and nitrite ( $\text{NO}_2^-$ -N) concentrations were administered as  $(\text{NH}_4)_2\text{SO}_4$ , and  $\text{NaNO}_2$ , respectively. The cathode chamber was filled with a mixture of potassium permanganate solution (10 mM) and phosphate buffer (50 mM, pH 7.0).

The anode chamber was continuously supplied with the wastewater using a peristaltic pump, and the hydraulic retention time (HRT) was set to 4 h. The ratio of  $\text{NH}_4^+$ -N to  $\text{NO}_2^-$ -N was fixed at 1:1.32, and the influent concentrations of  $\text{NH}_4^+$ -N and  $\text{NO}_2^-$ -N were varied along with the different operating periods. When the output voltage reached and remained at a relatively stable value for at least 6 HRT, it was considered that the MFC reached a steady state, then the influent concentration was raised to the next value. The catholyte was supplied using a peristaltic pump (5 mL/min). The anode and cathode electrolytes were bubbled with argon to remove oxygen before being mixed by a magnetic stirrer (HJ-2, Jin Tan Co., Ltd., Jintan, China) during the test. The anode anammox MFC was kept at  $30 \pm 1^\circ\text{C}$  in a biochemical incubator.

## 2.3. Analyses and Calculations

The ammonium–nitrogen ( $\text{NH}_4^+$ -N), nitrite–nitrogen ( $\text{NO}_2^-$ -N), nitrate–nitrogen ( $\text{NO}_3^-$ -N) and total nitrogen (TN) values were measured using the APHA Standard Methods [24]. The pH was determined by an S20 K pH meter (Mettler Toledo, Zurich, Switzerland). The conductivity was measured by an FE30 conductivity meter (Mettler Toledo, Zurich, Switzerland). The output voltages were recorded every 2 min by the DAS. The power density and the coulombic efficiency (CE) were calculated according to the methods outlined in previous studies [25]. The electrode potential was measured using an Ag/AgCl electrode (+0.195 V vs. SHE) as the reference electrode.

Polarization tests were performed with the gradual change ( $80,000 \Omega - 10 \Omega$ ) in the external resistance and the quasi-stable voltage, the anode potential and the cathode potential were recorded, and the current density was calculated. Polarization curves were plotted by taking the current density, the voltage, the anode potential, and the cathode potential as the ordinate and the current density as the abscissa [26]. A three-electrode system and a potentiostat (CHI660D, Beijing Huake Putian Technology Co., Ltd., Beijing, China) were used to perform electrochemical impedance spectroscopy (EIS) [27]. The sinusoidal disturbance voltage was 10 mV and the frequency range was  $10^{-3}$ – $10^5$  Hz. The EIS equivalent circuit was fitted by ZSimpWin3.10 software.

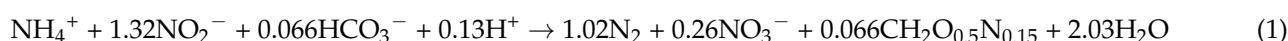
### 3. Results and Discussion

#### 3.1. Nitrogen Removal

The nitrogen removal performance of the anode anammox MFC under different nitrogen loads is shown in Figure 2. As the influent concentrations of  $\text{NH}_4^+$ -N and  $\text{NO}_2^-$ -N gradually elevated from 25 to 250 mg/L and 33–330 mg/L, respectively, the removal efficiencies of  $\text{NH}_4^+$ -N,  $\text{NO}_2^-$ -N and TN were over 90%, 90% and 80%, respectively (Figure 2A,B). Meanwhile, the volumetric nitrogen removal rate rose from  $0.32 \pm 0.05 \text{ kg N}/(\text{m}^3 \cdot \text{d})$  to a maximum of  $3.01 \pm 0.27 \text{ kg N}/(\text{m}^3 \cdot \text{d})$  (Figure 2C). However, when the influent  $\text{NH}_4^+$ -N and  $\text{NO}_2^-$ -N concentrations further increased to 300 mg/L and 396 mg/L, the nitrogen removal efficiencies suddenly declined and the effluent concentrations of  $\text{NH}_4^+$ -N and  $\text{NO}_2^-$ -N rose drastically to values almost equal to those of the influent (Figure 2A). Under these circumstances, the activities of anammox bacteria were fully inhibited [28]. The decrease in nitrogen removal in the anode anammox MFC indicated that the nitrogen load or nitrogen concentration had exceeded the maximum threshold value that the MFC could withstand.

Ammonium and nitrite are the two main substrates used by anammox bacteria, but they are potential inhibitors when their concentrations surpass the threshold inhibition values [29,30]. In order to reverse the self-inhibition at high nitrogen concentrations and increase microbial activity in the anode anammox MFC, the residual ammonium and nitrite were firstly washed out of the anode chamber, followed by a progressive increase in influent N concentrations, according to the remedial method of Tang et al. [28]. The nitrogen removal performance recovered after the remedial measures (Figure 2A,B).

When the anode anammox MFC ran stably, the ratio of the consumed  $\text{NO}_2^-$ -N to the consumed  $\text{NH}_4^+$ -N ranged from 1.25 to 1.40, and the ratio of the produced  $\text{NO}_3^-$ -N to the consumed  $\text{NH}_4^+$ -N was 0.15–0.23 (Figure 2D), which was close to the theoretical stoichiometry for the following anammox reaction (Equation (1)) [17]:



In addition, nitrate ( $\text{NO}_3^-$ ) was produced in the effluent. These results indicated that the anode nitrogen conversion in the MFC was in accordance with the typical anammox reaction. Owing to the faster oxidation rate of ammonium in the anammox process than in the nitrification process, the maximum volumetric nitrogen removal rate of the anode anammox MFC was  $3.01 \pm 0.27 \text{ kg N}/(\text{m}^3 \cdot \text{d})$ , which was much higher than that of anode nitrification MFCs ( $0.240 \text{ kg N}/(\text{m}^3 \cdot \text{d})$ ) [13,14] and previously reported anode anammox MFCs ( $0.417 \text{ kg N}/(\text{m}^3 \cdot \text{d})$ ) [20,21]. Considering that the inoculated anammox bacteria demonstrated very high nitrogen removal abilities, the potential nitrogen removal efficiency of the anode anammox MFC might be further improved under optimized operating conditions [18,31,32].

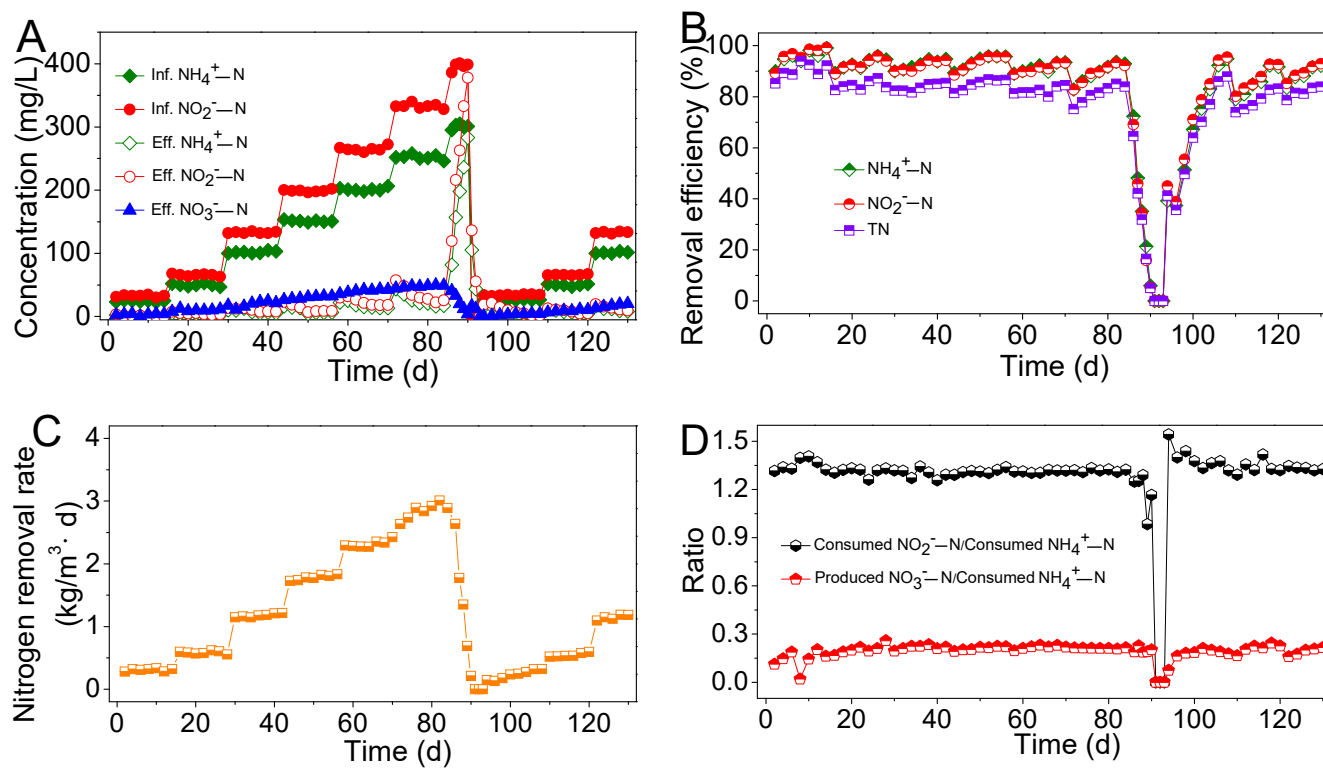


**Figure 2.** Nitrogen removal in the anode anammox MFC: (A) the concentrations of  $\text{NH}_4^+ \text{-N}$ ,  $\text{NO}_2^- \text{-N}$  and  $\text{NO}_3^- \text{-N}$  in the influent and effluent; (B) removal efficiency changes in  $\text{NH}_4^+ \text{-N}$ ,  $\text{NO}_2^- \text{-N}$  and TN; (C) variation in volumetric nitrogen removal rate over time and (D) ratio of consumed  $\text{NO}_2^- \text{-N}$  to consumed  $\text{NH}_4^+ \text{-N}$  and ratio of produced  $\text{NO}_3^- \text{-N}$  to consumed  $\text{NH}_4^+ \text{-N}$ .

### 3.2. Electricity Generation

The electricity generation performance of the anode anammox MFC under different nitrogen loads is depicted in Figure 3. The output voltage gradually increased from  $35.13 \pm 4.96 \text{ mV}$  to  $225.48 \pm 10.71 \text{ mV}$  as the influent nitrogen concentrations increased (Figure 3A). The power density of the anode anammox MFC also rose with escalating influent nitrogen concentrations and the maximum value reached  $1308.23 \pm 40.38 \text{ mW/m}^2$  (Figure 3B). The output voltage suffered a great loss following substrate self-inhibition and the electricity generation performance increased after the high nitrogen inhibition rate was counteracted (Figure 3A). Simultaneous change was observed between electricity generation and nitrogen removal, and Pearson correlation analysis was conducted to explore the relationship between them. Significant correlation between the maximum voltage and the volumetric nitrogen removal rate at each concentration was observed ( $R^2 = 0.9862$ ,  $p < 0.05$ ), which showed that electricity generation depends on ammonium oxidation in the anode anammox MFCs. The results corresponded well with reports that electrogensis from MFCs showed a meaningful relationship with substrate degradation [33,34].

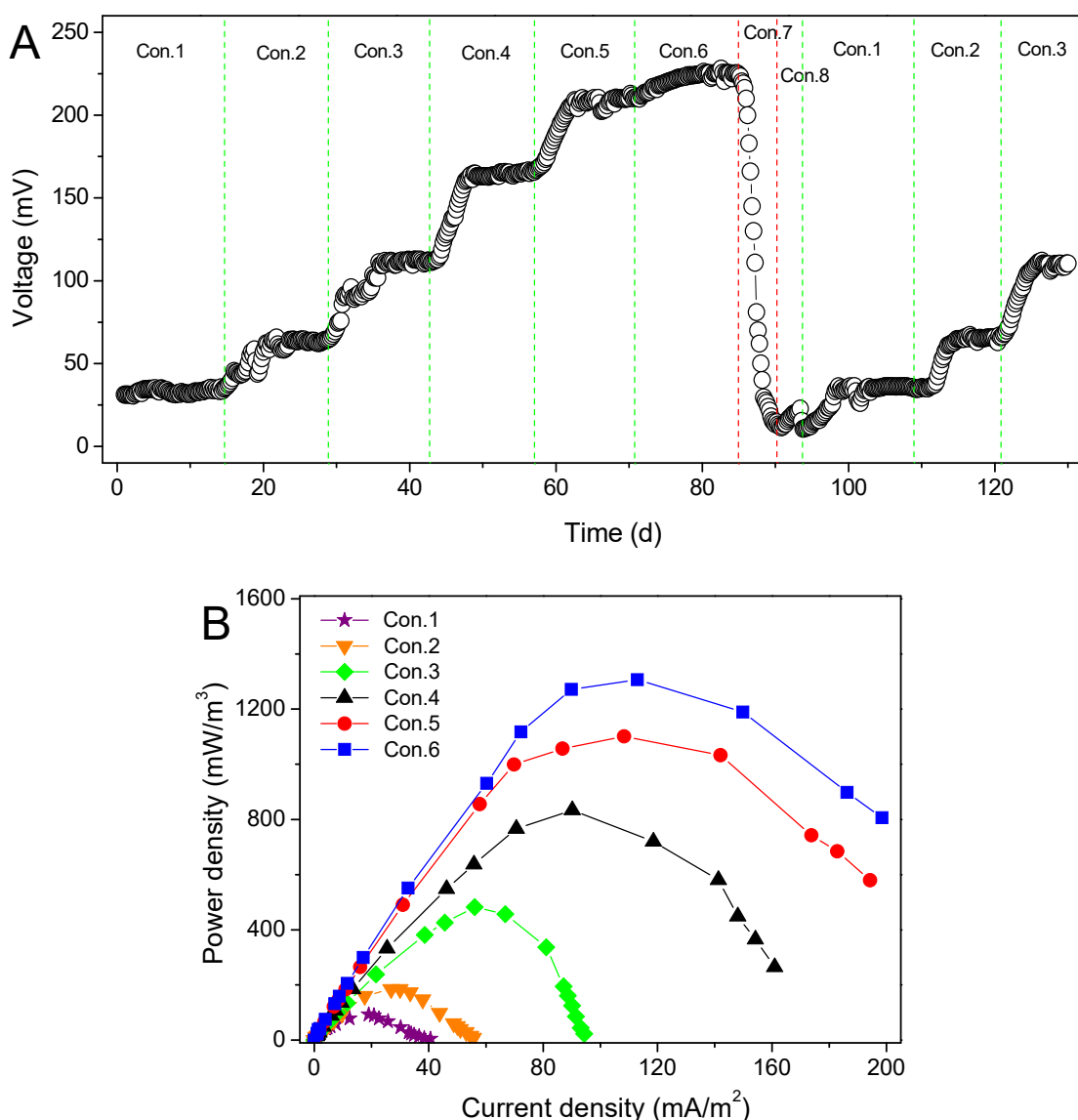


**Figure 3.** Profiles of (A) output voltage and (B) power density as a function of current output under different influent nitrogen concentrations ( $\text{NH}_4^+$ -N concentrations: Con.1: 25 mg/L, Con.2: 50 mg/L, Con.3: 100 mg/L, Con.4: 150 mg/L, Con.5: 200 mg/L, Con.6: 250 mg/L, Con.7: 300 mg/L; Con.8: 0 mg/L) in the anode anammox MFC.

By measuring the electrode potentials of the anode anammox MFC across different influent nitrogen concentrations, it was found that the cathode potential remained nearly stable (about 865 mV vs. SHE), while the anode potential gradually reduced with the rising nitrogen concentrations (Figure 4). The output voltage was the potential difference between the cathode and the anode, so the change in the output voltage was mainly caused by the evolution of the anode potential [35,36]. Coulomb efficiency (CE) is the ratio of electrons captured by the MFC for electricity production and the electrons derived from the oxidation of fuel, reflecting the utilization efficiency of fuel by the MFC [25]. The CE of the anode anammox MFC reduced from  $5.99 \pm 0.12\%$  to  $4.09 \pm 0.46\%$  with the increasing nitrogen concentrations (Figure 5). The utilization efficiency of fuel by the anode anammox MFC declined with the increase in substrate concentration, which was consistent with other reported studies [37,38].

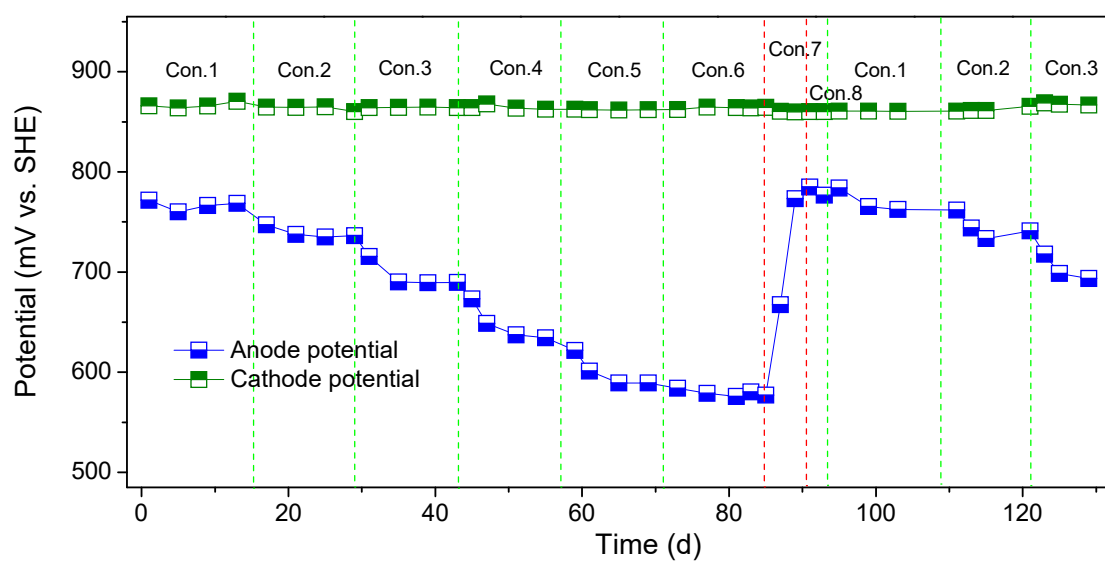


**Figure 4.** Variation in electrode potentials in the anode anammox MFC.

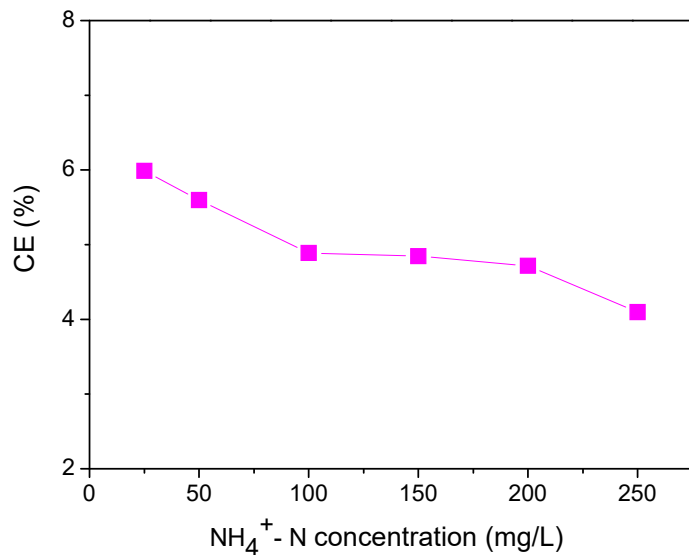


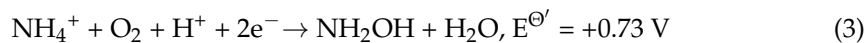
**Figure 5.** Change in CE with increasing influent concentrations.

The electricity generation performance of the anode anammox MFC was compared with other types of MFCs (Table 1). The anode anammox MFC had clear advantages over anode nitrification MFCs and previous anode anammox MFCs, while the electricity production parameters were lower than those for organic MFCs, especially for CE. In organic MFCs, the organic compounds are primarily consumed by electrogenic/non-electrogenic fermentation without exogenous electron acceptors and the anode potentials usually remain negative [39–42]. Therefore, the potential difference between the two electrodes is large, and the organic MFCs can produce more electric power [8,43–45]. With regard to ammonium-based bioelectrochemical systems, the oxidation of ammonium can be realized by two ways. The first method, in MFCs, is to add exogenous electron acceptors (oxygen or nitrite), which might compete with the anode for electrons, leading to low CE [13,14,20,21]. The second method, in MECs, is to place the anode at oxidative potentials (0.6 V vs. Ag/AgCl) [22,46,47].

**Table 1.** Comparison of electricity generation in the anode anammox MFC, anode nitrification MFC and Organic MFC.

MFC Types	Maximum Output Voltage (mV)	Maximum Power Density (mW/m <sup>3</sup> )	CE (%)	Anode Reactions and Potentials (vs. SHE)	References
Anode anammox MFC	225.48	1308.23 ± 40.38	4.09~5.99	① NO <sub>2</sub> <sup>-</sup> + 2H <sup>+</sup> + e <sup>-</sup> → NO + H <sub>2</sub> O ( $E^{\ominus'}$ = +0.38 V) ② NO + NH <sub>4</sub> <sup>+</sup> + 2H <sup>+</sup> + 3e <sup>-</sup> → N <sub>2</sub> H <sub>4</sub> + H <sub>2</sub> O ( $E^{\ominus'}$ = +0.06 V) ③ N <sub>2</sub> H <sub>4</sub> → N <sub>2</sub> + 4H <sup>+</sup> + 4e <sup>-</sup> ( $E^{\ominus'}$ = -0.75 V) ④ NO <sub>2</sub> <sup>-</sup> + H <sub>2</sub> O → NO <sub>3</sub> <sup>-</sup> + 2e <sup>-</sup> + 2H <sup>+</sup> ( $E^{\ominus'}$ = -0.43 V)	This research
	48	—	—	—	[20]
	201.6	90.3	—	—	[21]
Anode nitrification MFC	98.5	2.43 ± 0.07	0.31~1.1	① NH <sub>4</sub> <sup>+</sup> + O <sub>2</sub> + H <sup>+</sup> + 2e <sup>-</sup> → NH <sub>2</sub> OH + H <sub>2</sub> O ( $E^{\ominus'}$ = +0.73 V) ② NH <sub>2</sub> OH + H <sub>2</sub> O → NO <sub>2</sub> <sup>-</sup> + 5H <sup>+</sup> + 4e <sup>-</sup> ( $E^{\ominus'}$ = -0.06 V) ③ NO <sub>2</sub> <sup>-</sup> + H <sub>2</sub> O → NO <sub>3</sub> <sup>-</sup> + 2e <sup>-</sup> + 2H <sup>+</sup> ( $E^{\ominus'}$ = -0.43 V)	[13]
	82	93.3	—	—	[14]
Organic MFC	340	902.8	72.3	CH <sub>3</sub> COO <sup>-</sup> + 2H <sub>2</sub> O → 2CO <sub>2</sub> + 7H <sup>+</sup> + 8e <sup>-</sup> ( $E^{\ominus'}$ = -0.29 V)	[8]
	466	7250	71	—	[43]
	540	66,000	43	C <sub>6</sub> H <sub>12</sub> O <sub>6</sub> + 6H <sub>2</sub> O → 6CO <sub>2</sub> + 24H <sup>+</sup> + 24e <sup>-</sup> ( $E^{\ominus'}$ = -0.428 V)	[44]
	198	885 ± 346	59 ± 4	—	[45]

Both the nitrification process and the anammox process were multistage reactions, including positive potential and negative potential reaction steps (Table 1). Higher anode potentials are essential for ammonium oxidation but would be unfavorable for electricity generation. The anammox reactions demonstrated lower positive anode potential (Equation (2)) than that of the aerobic ammonia oxidation reactions (Equation (3)) [48], which might be the reason why the anode anammox MFC exhibited better performance in power generation than the anode nitrification MFCs.



### 3.3. Electrochemical Characteristics

The electrochemical characteristics of the anode anammox MFC were investigated in order to understand why those electrons released from the anammox process were not sufficiently utilized for electricity generation and led to losses of power output. The internal resistance of an MFC (mainly including activation loss, ohmic loss and mass transport loss) is closely related to the power output losses and polarization curves are useful tools for determining the resistance [25,26]. The polarization curves of the anode anammox MFC plotted at various influent concentrations are illustrated in Figure 6A. The slopes of the polarization curves in the low current density region were steep, indicating that the activation loss was significant while slow drops of the curves represented much a smaller ohmic loss and mass transport loss in the medium and high current density regions [25]. The polarization curves for different electrodes are depicted in Figure 6B. The cathode potentials reduced slowly with the increase in current density, and the cathodic polarization was not significant. By contrast, the variation in anode potentials was more visible than for the cathode potentials, especially in the low current density region, indicating that anodic polarization was more significant than cathodic polarization and activation loss was noted in the anodic electrochemical reaction [49,50]. Based on the above tests, the activation loss of the anode might be the main limiting factor for electricity generation in the anode anammox MFC.

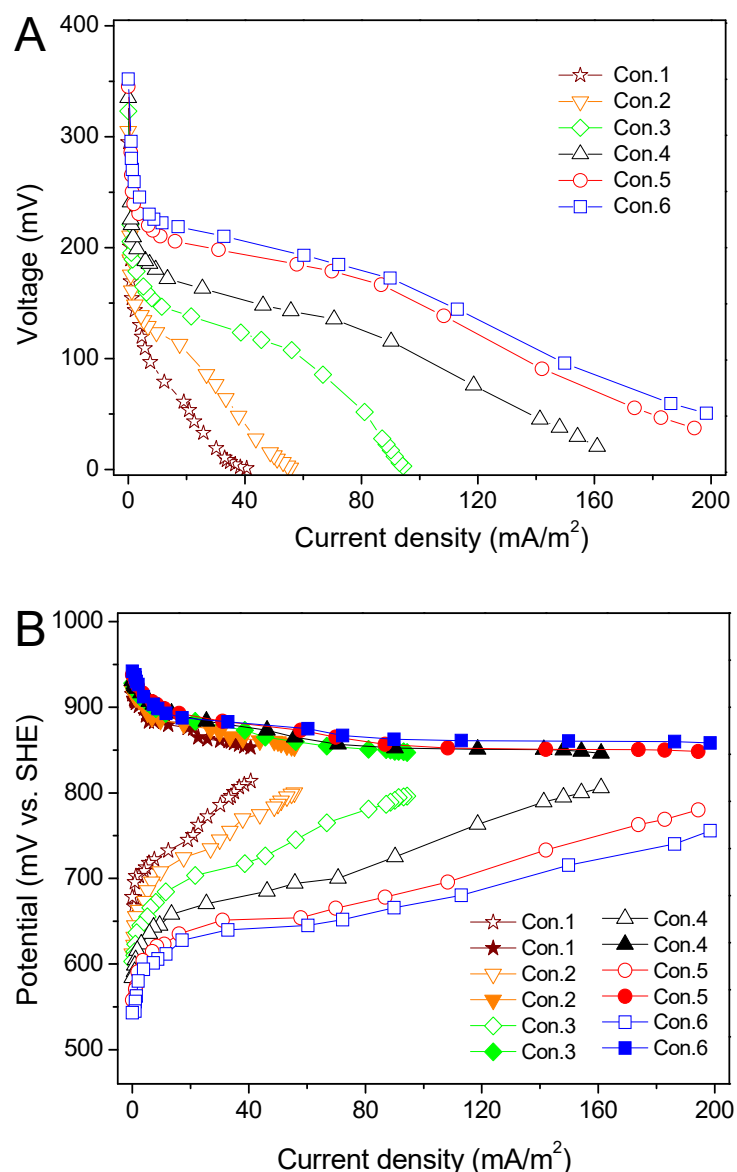


**Figure 6.** Polarization curves of (A) whole MFCs and (B) electrodes (cathode: filled symbols; anode: open symbols) under different influent concentrations (Con.1 to Con.6 represent  $\text{NH}_4^+ \text{-N}$  concentrations from 25 mg/L to 250 mg/L).

Electrochemical impedance spectroscopy (EIS) causes very little disturbance to the test system and is a non-destructive electrochemical test technology that can obtain data on MFC resistance and other important parameters under actual operating conditions [25,27]. In order to analyze in detail the anode process during ammonium oxidation, EIS was performed to quantify the different components of anode internal resistance ( $R_{in}$ ), including charge transfer resistance ( $R_{ct}$ ), ohmic resistance ( $R_o$ ) and diffusion resistance ( $R_d$ ) [27]. It can be observed that the plots were mainly composed of semicircles at the high frequencies (Figure 7), indicating that  $R_{ct}$  is the main type of anode resistance. The diameter of the semicircles decreased as the influent concentrations increased, showing that the  $R_{ct}$  reduced as the biochemical reaction rate increased [27,51]. The accurate results in Table 2 were obtained by fitting the Nyquist plot data to an appropriate equivalent circuit (Figure 8) using ZSimpWin3.10 software [52,53]. At each influent concentration, the resistance distribution of the anode was as follows:  $R_{ct}$  (90%)  $\gg R_o > R_d$ . The results indicated that the anode charge transfer resistance was mostly responsible for the anode anammox MFC internal resistance.

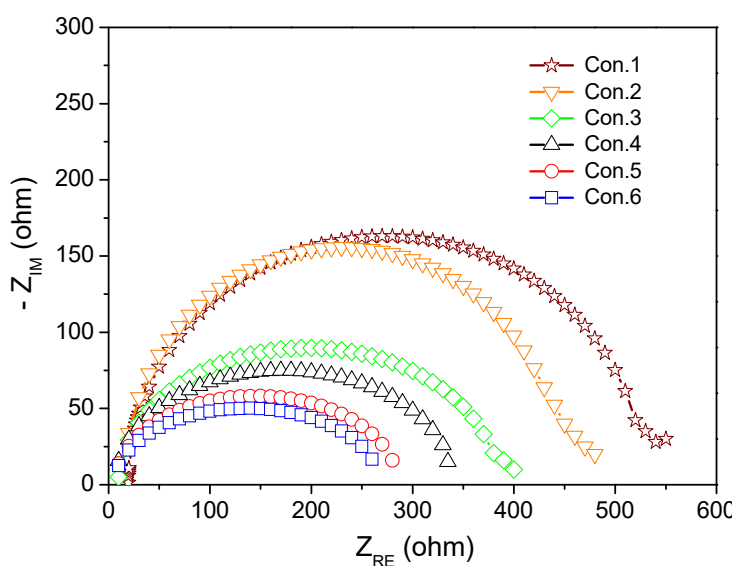


**Figure 7.** Nyquist plots of the anode under different influent concentrations.

**Table 2.** Resistance distribution of the anode obtained from the equivalent electrical circuit.

NH <sub>4</sub> <sup>+</sup> -N Concentration (mg/L)	R <sub>ct</sub> (Ω)	R <sub>o</sub> (Ω)	R <sub>d</sub> (Ω)	R <sub>ct</sub> /R <sub>in</sub> (%)
25	407.4 ± 15.3	19.4 ± 2.3	5.5 ± 0.9	68.2 ± 3.6
50	346.3 ± 6.4	14.8 ± 1.5	3.5 ± 1.1	66.1 ± 4.7
100	298.8 ± 7.2	9.7 ± 2.9	2.1 ± 0.8	65.2 ± 3.3
150	267.2 ± 2.8	6.3 ± 1.8	1.8 ± 0.6	68.1 ± 9.5
200	223.4 ± 9.1	6.0 ± 2.6	0.9 ± 0.2	59.7 ± 4.8
250	209.2 ± 3.4	5.9 ± 1.2	0.6 ± 0.1	58.6 ± 8.1

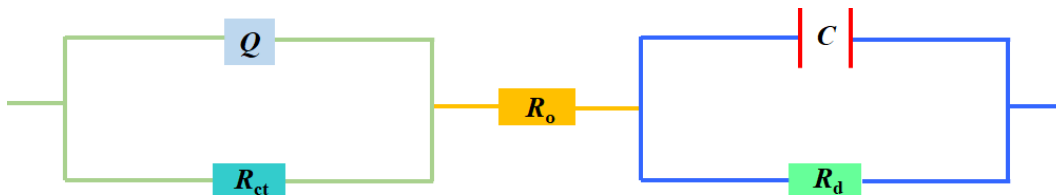


**Figure 8.** Equivalent electrical circuit for the electrochemical impedance spectra data simulation (Q is the constant phase element and C stands for double-layer capacitor).

The anode charge transfer resistance (or active resistance) is caused by the energy loss in the process of electron transfer from microbial cells to the electrode surface, and is affected by the kinetics of the electrode reactions [54,55]. Large anode charge transfer resistance generally means a low electron transfer rate or low electrode reaction rate [51,52]. Anammox bacteria were the main functional bacteria in the anode anammox MFC, whose cells possess a unique compartment structure called anammoxosome. The anammox reaction takes place inside the anammoxosome bounded by a low-permeability ladderane lipid-containing membrane, decreasing its permeability to protons and hydrazine. Additionally, the anammoxosome was also enclosed by the intracytoplasmic membrane and cytoplasmic membrane [17]. Compared with other reported electrochemically active bacteria [56], an additional electron transfer barrier (the anammoxosome compartment) must be crossed by anammox bacteria to transfer the electrons and the unique cell structure might hinder extracellular electron transfer [22], which was in accordance with the large anode charge transfer resistance in our study. The performance of the anode might be improved

by selecting materials with better electrical properties (such as coated carbon nanotubes), adding artificial electron mediators in the electrolyte or even editing bacterial genes related to the electron transport chain to minimize the electron transfer resistance and reinforce the electricity generation performance of the anode anammox MFCs [57–59]. In fact, the anode electricity generation process in the anode anammox MFC is a new complex microbial and bioelectrochemical reaction. More in-depth study of the underlying interaction between microorganisms and electrodes during the electricity generating process, and the reaction kinetics or the effect of bacterial metabolism on electrodes, in future can help to further improve the process.

#### 4. Conclusions

The emergence of ammonium-based MFCs provided an alternative approach for sustainable nitrogen-containing wastewater treatment. An anode anammox MFC developed by highly effective anammox bacteria showed stable nitrogen removal and electricity generation under different nitrogen concentrations during a long-term operation. It showed excellent nitrogen removal performance with a maximum volumetric nitrogen removal rate of  $3.01 \pm 0.27 \text{ kg N}/(\text{m}^3 \cdot \text{d})$ . It also presented certain electricity recovery potential with a maximum power density of  $1308.23 \pm 40.38 \text{ mW/m}^3$ . Compared with the previous anode nitrification MFCs, the anode anammox MFC achieved much higher nitrogen removal and electricity generation performance. The performance of the anode anammox MFC was significantly influenced by nitrogen concentration. The main challenge for the anode anammox MFC was low energy recovery efficiency. Substantial power losses were due to the anodic overpotential and the anode charge transfer resistance was the main reason for the internal resistance. To further reduce the anode charge transfer resistance in the anode anammox MFC, a better understanding of the whole process of the extracellular electron transfer between microorganisms and electrodes is essential in future studies.

**Author Contributions:** J.L. and P.Z.: conceptualization, obtained research funding, and editing; J.Z. and J.R.: software, data analysis, and writing—original draft preparation; Z.Z. and H.G.: review and editing; K.R., J.C., Y.X., L.R. and T.W.: investigation and validation. All authors have read and agreed to the published version of the manuscript.

**Funding:** This work was supported by the Natural Science Foundation of Shandong Province (ZR2019QEE039) and the National Natural Science Foundation of China (52070163 and 41977124).

**Data Availability Statement:** Not applicable.

**Conflicts of Interest:** The authors declare no conflict of interest.

#### References

- Logan, B.E.; Rabaey, K. Conversion of Wastes into Bioelectricity and Chemicals by Using Microbial Electrochemical Technologies. *Science* **2012**, *337*, 686–690. [[CrossRef](#)]
- McCarty, P.L.; Bae, J.; Kim, J. Domestic Wastewater Treatment as a Net Energy Producer—Can This be Achieved? *Environ. Sci. Technol.* **2011**, *45*, 7100–7106. [[CrossRef](#)] [[PubMed](#)]
- Heidrich, E.S.; Curtis, T.P.; Dolfig, J. Determination of the Internal Chemical Energy of Wastewater. *Environ. Sci. Technol.* **2011**, *45*, 827–832. [[CrossRef](#)] [[PubMed](#)]
- Rozendal, R.A.; Hamelers, H.; Rabaey, K.; Keller, J.; Buisman, C.J. Towards practical implementation of bioelectrochemical wastewater treatment. *Trends Biotechnol.* **2008**, *26*, 450–459. [[CrossRef](#)]
- Logan, B.E.; Regan, J.M. Microbial Fuel Cells—Challenges and Applications. *Environ. Sci. Technol.* **2006**, *40*, 5172–5180. [[CrossRef](#)]
- Li, W.-W.; Yu, H.-Q.; He, Z. Towards sustainable wastewater treatment by using microbial fuel cells-centered technologies. *Energy Environ. Sci.* **2014**, *7*, 911–924. [[CrossRef](#)]
- Bond, D.R.; Holmes, D.E.; Tender, L.M.; Lovley, D.R. Electrode-Reducing Microorganisms That Harvest Energy from Marine Sediments. *Science* **2002**, *295*, 483–485. [[CrossRef](#)]
- Chae, K.-J.; Choi, M.-J.; Lee, J.-W.; Kim, K.-Y.; Kim, I.S. Effect of different substrates on the performance, bacterial diversity, and bacterial viability in microbial fuel cells. *Bioresour. Technol.* **2009**, *100*, 3518–3525. [[CrossRef](#)]
- Pandey, P.; Shinde, V.N.; Deopurkar, R.L.; Kale, S.P.; Patil, S.A.; Pant, D. Recent advances in the use of different substrates in microbial fuel cells toward wastewater treatment and simultaneous energy recovery. *Appl. Energy* **2016**, *168*, 706–723. [[CrossRef](#)]

10. Kelly, P.T.; He, Z. Nutrients removal and recovery in bioelectrochemical systems: A review. *Bioresour. Technol.* **2014**, *153*, 351–360. [[CrossRef](#)]
11. Virdis, B.; Rabaey, K.; Rozendal, R.A.; Yuan, Z.; Keller, J. Simultaneous nitrification, denitrification and carbon removal in microbial fuel cells. *Water Res.* **2010**, *44*, 2970–2980. [[CrossRef](#)] [[PubMed](#)]
12. Park, Y.; Park, S.; Nguyen, V.K.; Yu, J.; Torres, C.I.; Rittmann, B.E.; Lee, T. Complete nitrogen removal by simultaneous nitrification and denitrification in flat-panel air-cathode microbial fuel cells treating domestic wastewater. *Chem. Eng. J.* **2017**, *316*, 673–679. [[CrossRef](#)]
13. He, Z.; Kan, J.; Wang, Y.; Huang, Y.; Mansfeld, F.; Nealson, K.H. Electricity Production Coupled to Ammonium in a Microbial Fuel Cell. *Environ. Sci. Technol.* **2009**, *43*, 3391–3397. [[CrossRef](#)]
14. Xie, Z.; Chen, H.; Zheng, P.; Zhang, J.; Cai, J.; Abbas, G. Influence and mechanism of dissolved oxygen on the performance of Ammonia-Oxidation Microbial Fuel Cell. *Int. J. Hydrogen Energy* **2013**, *38*, 10607–10615. [[CrossRef](#)]
15. Quan, X.-C.; Quan, Y.-P.; Tao, K. Effect of anode aeration on the performance and microbial community of an air–cathode microbial fuel cell. *Chem. Eng. J.* **2012**, *210*, 150–156. [[CrossRef](#)]
16. Kuypers, M.M.M.; Marchant, H.K.; Kartal, B. The microbial nitrogen-cycling network. *Nat. Rev. Microbiol.* **2018**, *16*, 263–276. [[CrossRef](#)] [[PubMed](#)]
17. Kartal, B.; Maalcke, W.J.; de Almeida, N.M.; Cirpus, I.; Gloerich, J.; Geerts, W.; Op den Camp, H.J.M.; Harhangi, H.R.; Janssen-Megens, E.M.; Francoijns, K.-J.; et al. Molecular mechanism of anaerobic ammonium oxidation. *Nature* **2011**, *479*, 127–130. [[CrossRef](#)] [[PubMed](#)]
18. Tang, C.-J.; Zheng, P.; Wang, C.-H.; Mahmood, Q.; Zhang, J.-Q.; Chen, X.-G.; Zhang, L.; Chen, J.-W. Performance of high-loaded ANAMMOX UASB reactors containing granular sludge. *Water Res.* **2011**, *45*, 135–144. [[CrossRef](#)]
19. Du, R.; Cao, S.; Li, B.; Niu, M.; Wang, S.; Peng, Y. Performance and microbial community analysis of a novel DEAMOX based on partial-denitrification and anammox treating ammonia and nitrate wastewaters. *Water Res.* **2017**, *108*, 46–56. [[CrossRef](#)]
20. Xu, M.Y.; Zhou, S.Q.; Liu, Z.J.; Wang, J.P.; Ma, F.Z. Study on performance of dual-chamber MFC coupled with Anammox process in a high nitrogen load circumstance. *Acta Sci. Circumstant.* **2017**, *37*, 154–161. (In Chinese)
21. Zu, B.; Ma, L.; Liu, B.; Lu, P.-L.; Xu, J. Effects of Organic Substrates on ANAMMOX-MFC Denitrification Electrogenesis Performance. *Environ. Sci.* **2018**, *39*, 3937–3945.
22. Shaw, D.R.; Ali, M.; Katuri, K.P.; Gralnick, J.A.; Reimann, J.; Mesman, R.; van Niftrik, L.; Jetten, M.S.M.; Saikaly, P.E. Extracellular electron transfer-dependent anaerobic oxidation of ammonium by anammox bacteria. *Nat. Commun.* **2020**, *11*, 2058. [[CrossRef](#)]
23. Zhang, J.; Zheng, P.; Zhang, M.; Chen, H.; Chen, T.; Xie, Z.; Cai, J.; Abbas, G. Kinetics of substrate degradation and electricity generation in anodic denitrification microbial fuel cell (AD-MFC). *Bioresour. Technol.* **2013**, *149*, 44–50. [[CrossRef](#)] [[PubMed](#)]
24. American Public Health Association (APHA). *Standard Methods for the Examination of Water and Wastewater*, 21st ed.; American Public Health Association: Washington, DC, USA, 2005; ISBN 087-553-047-8.
25. Logan, B.E.; Hamelers, B.; Rozendal, R.; Schröder, U.; Keller, J.; Freguia, S.; Aelterman, P.; Verstraete, W.; Rabaey, K. Microbial Fuel Cells: Methodology and Technology. *Environ. Sci. Technol.* **2006**, *40*, 5181–5192. [[CrossRef](#)] [[PubMed](#)]
26. Wang, B.; Han, J.-I. A single chamber stackable microbial fuel cell with air cathode. *Biotechnol. Lett.* **2009**, *31*, 387–393. [[CrossRef](#)] [[PubMed](#)]
27. Manohar, A.K.; Bretschger, O.; Nealson, K.H.; Mansfeld, F. The use of electrochemical impedance spectroscopy (EIS) in the evaluation of the electrochemical properties of a microbial fuel cell. *Bioelectrochemistry* **2008**, *72*, 149–154. [[CrossRef](#)] [[PubMed](#)]
28. Tang, C.-J.; Zheng, P.; Mahmood, Q.; Chen, J.-W. Start-up and inhibition analysis of the Anammox process seeded with anaerobic granular sludge. *J. Ind. Microbiol. Biotechnol.* **2009**, *36*, 1093–1100. [[CrossRef](#)] [[PubMed](#)]
29. Jin, R.-C.; Yang, G.-F.; Yu, J.-J.; Zheng, P. The inhibition of the Anammox process: A review. *Chem. Eng. J.* **2012**, *197*, 67–79. [[CrossRef](#)]
30. Hong, S.; De Clippeleir, H.; Goel, R. Response of mixed community anammox biomass against sulfide, nitrite and recalcitrant carbon in terms of inhibition coefficients and functional gene expressions. *Chemosphere* **2022**, *308*, 136232. [[CrossRef](#)]
31. Li, Y.-Y.; Huang, X.-W.; Li, X.-Y. Use of a packed-bed biofilm reactor to achieve rapid formation of anammox biofilms for high-rate nitrogen removal. *J. Clean. Prod.* **2021**, *321*, 128999. [[CrossRef](#)]
32. Li, B.; Wang, Y.; Wang, W.; Huang, X.; Kou, X.; Wu, S.; Shao, T. High-rate nitrogen removal in a continuous biofilter anammox reactor for treating low-concentration nitrogen wastewater at moderate temperature. *Bioresour. Technol.* **2021**, *337*, 125496. [[CrossRef](#)] [[PubMed](#)]
33. Juang, D.-F.; Yang, P.-C.; Chou, H.-Y.; Chiu, L.-J. Effects of microbial species, organic loading and substrate degradation rate on the power generation capability of microbial fuel cells. *Biotechnol. Lett.* **2011**, *33*, 2147–2160. [[CrossRef](#)] [[PubMed](#)]
34. Cai, J.; Qaisar, M.; Sun, Y.; Wang, K.; Lou, J.; Wang, R. Coupled substrate removal and electricity generation in microbial fuel cells simultaneously treating sulfide and nitrate at various influent sulfide to nitrate ratios. *Bioresour. Technol.* **2020**, *306*, 123174. [[CrossRef](#)]
35. Wei, J.; Liang, P.; Cao, X.; Huang, X. A New Insight into Potential Regulation on Growth and Power Generation of *Geobacter sulfurreducens* in Microbial Fuel Cells Based on Energy Viewpoint. *Environ. Sci. Technol.* **2010**, *44*, 3187–3191. [[CrossRef](#)] [[PubMed](#)]
36. Lu, M.; Qian, Y.; Huang, L.; Xie, X.; Huang, W. Improving the performance of microbial fuel cells through anode manipulation. *ChemPlusChem* **2015**, *80*, 1216–1225. [[CrossRef](#)] [[PubMed](#)]

37. Gao, Y.; Yin, F.; Ma, W.; Wang, S.; Liu, Y.; Liu, H. Rapid detection of biodegradable organic matter in polluted water with microbial fuel cell sensor: Method of partial coulombic yield. *Bioelectrochemistry* **2020**, *133*, 107488. [[CrossRef](#)]
38. Jadhav, G.; Ghangrekar, M. Performance of microbial fuel cell subjected to variation in pH, temperature, external load and substrate concentration. *Bioresour. Technol.* **2009**, *100*, 717–723. [[CrossRef](#)]
39. Logan, B.E. Exoelectrogenic bacteria that power microbial fuel cells. *Nat. Rev. Microbiol.* **2009**, *7*, 375–381. [[CrossRef](#)]
40. de los Ángeles Fernandez, M.; de los Ángeles Sanromán, M.; Marks, S.; Makinia, J.; Del Campo, A.G.; Rodrigo, M.; Fernandez, F.J. A grey box model of glucose fermentation and syntrophic oxidation in microbial fuel cells. *Bioresour. Technol.* **2016**, *200*, 396–404. [[CrossRef](#)]
41. Mei, X.; Lu, B.; Yan, C.; Gu, J.; Ren, N.; Ren, Z.J.; Xing, D. The interplay of active energy harvesting and wastewater organic loading regulates fermentation products and microbiomes in microbial fuel cells. *Resour. Conserv. Recycl.* **2022**, *183*, 106366. [[CrossRef](#)]
42. Esquivel, D.Y.A.; Guo, Y.; Brown, R.K.; Müller, S.; Schröder, U.; Harnisch, F. Investigating Community Dynamics and Performance During Microbial Electrochemical Degradation of Whey. *ChemElectroChem* **2020**, *7*, 989–997. [[CrossRef](#)]
43. Lee, H.-S.; Parameswaran, P.; Kato-Marcus, A.; Torres, C.I.; Rittmann, B.E. Evaluation of energy-conversion efficiencies in microbial fuel cells (MFCs) utilizing fermentable and non-fermentable substrates. *Water Res.* **2008**, *42*, 1501–1510. [[CrossRef](#)] [[PubMed](#)]
44. Rabaey, K.; Clauwaert, P.; Aelterman, P.; Verstraete, W. Tubular Microbial Fuel Cells for Efficient Electricity Generation. *Environ. Sci. Technol.* **2005**, *39*, 8077–8082. [[CrossRef](#)] [[PubMed](#)]
45. Kim, K.-Y.; Chae, K.-J.; Choi, M.-J.; Ajayi, F.F.; Jang, A.; Kim, C.-W.; Kim, I.S. Enhanced Coulombic efficiency in glucose-fed microbial fuel cells by reducing metabolite electron losses using dual-anode electrodes. *Bioresour. Technol.* **2011**, *102*, 4144–4149. [[CrossRef](#)]
46. Vilajeliu-Pons, A.; Koch, C.; Balaguer, M.D.; Colprim, J.; Harnisch, F.; Puig, S. Microbial electricity driven anoxic ammonium removal. *Water Res.* **2018**, *130*, 168–175. [[CrossRef](#)]
47. Qu, B.; Fan, B.; Zhu, S.; Zheng, Y. Anaerobic ammonium oxidation with an anode as the electron acceptor. *Environ. Microbiol. Rep.* **2014**, *6*, 100–105. [[CrossRef](#)]
48. Jetten, M.S.M.; Van Niftrik, L.; van Strous, M.; Kartal, B.; Keltjens, J.T.; op den Camp, H.J.M. Biochemistry and molecular biology of anammox bacteria. *Crit. Rev. Biochem. Mol. Biol.* **2009**, *44*, 65–84. [[CrossRef](#)]
49. Manohar, A.K.; Bretschger, O.; Nealson, K.H.; Mansfeld, F. The polarization behavior of the anode in a microbial fuel cell. *Electrochim. Acta* **2008**, *53*, 3508–3513. [[CrossRef](#)]
50. Zhang, Y.; Mo, G.; Li, X.; Zhang, W.; Zhang, J.; Ye, J.; Huang, X.; Yu, C. A graphene modified anode to improve the performance of microbial fuel cells. *J. Power Sources* **2011**, *196*, 5402–5407. [[CrossRef](#)]
51. He, Z.; Mansfeld, F. Exploring the use of electrochemical impedance spectroscopy (EIS) in microbial fuel cell studies. *Energy Environ. Sci.* **2009**, *2*, 215–219. [[CrossRef](#)]
52. Wang, H.; Long, X.; Sun, Y.; Wang, D.; Wang, Z.; Meng, H.; Jiang, C.; Dong, W.; Lu, N. Electrochemical impedance spectroscopy applied to microbial fuel cells: A review. *Front. Microbiol.* **2022**, *13*, 973501. [[CrossRef](#)]
53. Sindhuja, M.; Kumar, N.S.; Sudha, V.; Harinipriya, S. Equivalent circuit modeling of microbial fuel cells using impedance spectroscopy. *J. Energy Storage* **2016**, *7*, 136–146. [[CrossRef](#)]
54. Shi, L.; Dong, H.; Reguera, G.; Beyenal, H.; Haluk, B.; Liu, J.; Yu, H.-Q.; Fredrickson, J.K. Extracellular electron transfer mechanisms between microorganisms and minerals. *Nat. Rev. Microbiol.* **2016**, *14*, 651–662. [[CrossRef](#)] [[PubMed](#)]
55. Light, S.H.; Su, L.; Rivera-Lugo, R.; Cornejo, J.A.; Louie, A.; Iavarone, A.T.; Ajo-Franklin, C.M.; Portnoy, D.A. A flavin-based extracellular electron transfer mechanism in diverse Gram-positive bacteria. *Nature* **2018**, *562*, 140–144. [[CrossRef](#)] [[PubMed](#)]
56. Hirose, A.; Kouzuma, A.; Watanabe, K. Towards development of electrogenetics using electrochemically active bacteria. *Biotechnol. Adv.* **2019**, *37*, 107351. [[CrossRef](#)] [[PubMed](#)]
57. Sonawane, J.M.; Yadav, A.; Ghosh, P.C.; Adeloju, S.B. Recent advances in the development and utilization of modern anode materials for high performance microbial fuel cells. *Biosens. Bioelectron.* **2017**, *90*, 558–576. [[CrossRef](#)]
58. Kumar, R.; Singh, L.; Zularisam, A. Exoelectrogens: Recent advances in molecular drivers involved in extracellular electron transfer and strategies used to improve it for microbial fuel cell applications. *Renew. Sustain. Energy Rev.* **2016**, *56*, 1322–1336. [[CrossRef](#)]
59. Xie, R.; Wang, S.; Wang, K.; Wang, M.; Chen, B.; Wang, Z.; Tan, T. Improved energy efficiency in microbial fuel cells by bioethanol and electricity co-generation. *Biotechnol. Biofuels* **2022**, *15*, 84. [[CrossRef](#)]